



The trajectory of landcover change in peatland complexes with discontinuous permafrost, northwestern Canada

Olivia Carpino^{1*}, Kristine Haynes¹, Ryan Connon², James Craig³, Élise Devoie³ and William Quinton¹

- 5 ¹*Cold Regions Research Centre, Wilfrid Laurier University, Waterloo, Ontario, N2L 3C5, CANADA*
²*Environment and Natural Resources, Government of the Northwest Territories, Yellowknife, Northwest Territories, X1A 2L9, CANADA*
³*Department of Civil and Environmental Engineering, University of Waterloo, Waterloo, Ontario, N2L 3G1, CANADA*
10 ^{*}*Corresponding author contact information: ocarpino@wlu.ca (519-884-1970)*

Abstract

The discontinuous permafrost zone is undergoing rapid transformation as a result of unprecedented permafrost thaw brought on by circumpolar climate warming. Rapid climate warming over recent decades has significantly decreased the area underlain by permafrost in peatland complexes. It has catalyzed extensive landscape transitions in the Taiga Plains of northwestern Canada, transforming forest-dominated landscapes to those that are wetland-dominated. The high rate and large spatial extent of this thaw-induced landcover transformation indicates that this region is particularly sensitive to warming temperatures and will continue to respond to climatic changes and landscape disturbances. This study explores the current trajectory of landcover change across a 300,000 km² region of northwestern Canada's discontinuous permafrost zone by presenting a space-for-time substitution that capitalizes on the region's 600 km latitudinal span. To illustrate this trajectory of change we present the distribution of peatland-rich environments that govern permafrost coverage in this region of the discontinuous permafrost zone. We also establish that relatively undisturbed forested plateau-wetland complexes dominate the region's higher latitudes, forest-wetland patchworks are most prevalent at the medial latitudes, and forested peatlands are increasingly present across lower latitudes, indicating not only a climatic gradient but also a landscape in transition as local mean temperatures increase. This study combines extensive geomatics data with ground-based meteorological and hydrological measurements to inform a new conceptual model of landscape evolution that accounts for the observed patterns of permafrost thaw-induced landcover change, and provides a basis for predicting future changes.

30 **Keywords:** discontinuous permafrost zone; Taiga Plains; peatland; climate change; boreal forest; hydrology; energy dynamics

Key Points

1. Geomatics methods are used to generate a distribution of peatland-dominated landscapes in the discontinuous permafrost zone
2. A conceptual model presents landscape evolution in peatland complexes following permafrost thaw
- 35 3. A space-for-time approach extrapolates landcover, energy, and water balance field data from the Scotty Creek Research Station to the regional landscape change anticipated across the Taiga Plains.



1. Introduction

Arctic and subarctic regions are undergoing unprecedented rates of climate warming and
40 as a result, these regions are experiencing widespread permafrost thaw (Overland et al. 2019).
Permafrost thaw is one of the most dramatic manifestations of climate warming and has the
potential to drastically change the biophysical features of the land surface. The rate, pattern, and
subsequent stages of thaw-driven landcover change across the circumpolar north are not well
understood. As a result, land and water resources in these regions have uncertain futures. This is
45 particularly evident across the discontinuous permafrost zone where substantial changes to
landcover (Quinton et al. 2011; Chasmer and Hopkinson 2017) and regional hydrology (Connon
et al. 2014; Korosi et al. 2017; Walvoord et al. 2019) have been documented.

While permafrost (*i.e.* perennially cryotic ground) underlies 16% of the Earth's land
surface (Tarnocai 2009), it is estimated that 80% of the world's boreal forest lies within this
50 circumpolar permafrost zone (Helbig et al. 2016a). In the southern extensive discontinuous and
sporadic discontinuous permafrost zones in the Taiga Plains ecoregion of northwestern Canada,
permafrost is preferentially located in low-lying, peatland-dominated areas. Such areas are
typically composed of raised, black spruce (*Picea mariana*) covered peat plateaus overlying thin
(<10 m), ice-rich permafrost; and permafrost-free treeless wetlands, including channel fens and
55 collapse scars, the latter of which result from thermokarst erosion of peat plateaus (Zoltai &
Tarnocai 1975; Robinson 2002; Carpino et al. 2018). The peat plateaus and collapsed wetlands
are arranged into distinct "plateau-wetland complexes" separated by channel fens.

Permafrost temperatures in the Taiga Plains have been warming steadily over the last
several decades (Kokelj et al. 2017; Holloway & Lewkowiz 2019). While permafrost throughout
60 the southern discontinuous permafrost zones is preferentially located in areas of high peatland



coverage due to the insulating properties of peat (Camill 1999), the observed rapid increases in air temperature, and consequently ground temperature, have initiated and accelerated permafrost thaw (Overland et al. 2019; Schuur, 2019). Specifically, the frozen ground along the southernmost boundary of the sporadic discontinuous permafrost zone is already at or very near
65 to the 0°C freezing point (Kwong & Gan 1994); indicating a state of disequilibrium with the current climate (Helbig et al. 2016a). While this condition occurs predominantly along the southern margin of permafrost, permafrost throughout the discontinuous zone can also be similarly warm (*i.e.* > -1°C) and vulnerable to thaw and degradation, particularly when vegetation is disturbed by anthropogenic (Smith et al. 2008; Smith & Riseborough 2010) or
70 natural (*e.g.* fire) causes (Gibson et al. 2018). Further north, permafrost in the extensive discontinuous zone is warming, but has not been documented to reach the temperatures found further south (Smith et al. 2005). While the northern portion of extensive discontinuous permafrost is not as immediately vulnerable to the thaw and degradation widely documented across the southern discontinuous zones, the conditions that occur there may provide insight into
75 the future conditions of northern environments as pan-Arctic warming continues.

The thaw of permafrost below plateaus is driven horizontally by conduction and advection from the adjacent wetlands, and vertically by conduction from the ground heat flux (Kurylyk et al. 2016). As permafrost thaws, the overlying plateau ground surface subsides and is engulfed by the surrounding wetlands (Helbig et al. 2016a). As such, permafrost thaw transforms
80 forested landcovers into treeless, permafrost-free wetlands (Quinton et al. 2011; Baltzer et al. 2014; Carpino et al. 2018). Zoltai (1993) envisioned this permafrost loss as part of a cyclical process that also includes regrowth, suggesting that the collapse scar wetland is both the end-point of permafrost loss and the starting point of permafrost regrowth. This cyclical progression



has now been disrupted by climate warming such that rates of permafrost loss greatly exceed
85 those of permafrost growth (Robinson & Moore 2000; Jorgenson et al. 2010; Chasmer &
Hopkinson 2017). However, the absence of permafrost regrowth does not preclude the re-
establishment of a black spruce forest (Haynes et al. under review; Chasmer & Hopkinson 2017).
Collapse scar wetlands have been found to revert to such a forest within two or three decades
where the raised permafrost on the wetland margins thaws, allowing the wetland to partially
90 drain, which is sufficient to allow for root establishment (Haynes et al. 2018; Haynes et al. under
review).

In the Taiga Plains between 55.5° N and 64.6° N, Beilman and Robinson (2003) reported
a 10 to 51% reduction in peat plateaus and thus, the area underlain by permafrost over 50 years.
In recent decades, accelerated thaw rates (Overland et al. 2019; Schuur, 2019; Biskaborn et al.
95 2019) have fragmented landcovers, profoundly impacting the flux and storage of water (Connon
et al. 2015) and energy (Kurylyk et al. 2016; Devoie et al. 2019). Presently, thermokarst
wetlands occupy more than 60% of the landscape in much of the peatland dominated lowlands of
the Taiga Plains (Olefeldt et al. 2016). Permafrost thaw is generally expected to intensify the
hydrological cycle of high latitude drainage basins (DeAngelis et al. 2015; Box et al. 2019).
100 Since peat plateaus, collapsed wetlands and channel fens are known to have contrasting
hydrological functions (Hayashi et al. 2004), the permafrost thaw driven change to their relative
cover (Quinton et al. 2011) combined with increased hydrological connectivity of the landscape
(Connon et al. 2015) has been documented to alter the flux and storage of water over the
landscape. Moreover, the reduction in the areal cover of forested plateaus and concomitant
105 increase in tree-free wetland cover alters ground surface energy partitioning (Kurylyk et al. 2016;
Devoie et al. 2019). The nature of these changes to a landscape's energy balance is governed by
properties of the subsurface, ground surface and the overlying canopy, all of which change as a



plateau transitions to a wetland (Helbig et al. 2016b). For example, insolation at the ground surface of a mature conifer canopy is roughly one order of magnitude less than for an open
110 ground surface (Pomeroy et al. 2003) such as a treeless wetland. The low albedo surfaces of the trunks, branches and stems on plateaus receive significant net shortwave, resulting in relatively high energy contributions of long-wave emission and sensible heat advection to the plateau ground surface compared to adjacent wetland surfaces (Helbig et al. 2016b).

This study examines peat plateau-wetland complexes along a latitudinal gradient through
115 the Taiga Plains in order to improve our understanding of permafrost thaw-driven landcover change in this region as well as advance our ability to predict changes over the coming decades. In light of this goal, the specific objectives of this work are to: (1) delineate the current extent of peatlands, permafrost, and forest distribution along the latitudinal gradient extending through the zones of discontinuous permafrost; (2) characterise end-members and intervening stages of
120 landcover transition; (3) for each stage identified, provide an interpretation of the hydrological and ground surface energy balance regimes based on twenty years of field studies at the Scotty Creek Research Station; and (4) present a conceptual model of peatland transition during and following permafrost thaw.

2. Methods

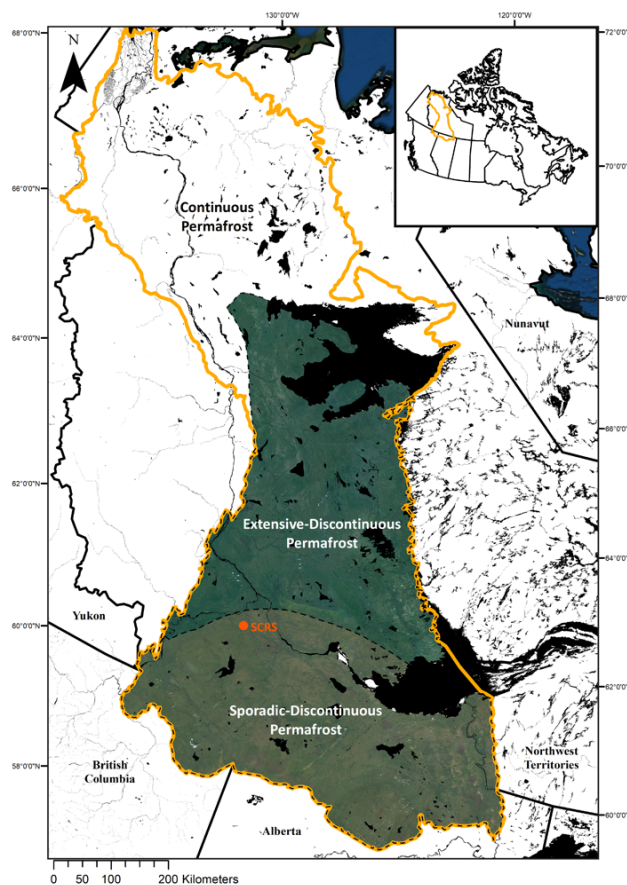
125 2.1 Study Region

Much of northwestern Canada's boreal ecoregion is located within the discontinuous permafrost zone, which ranges latitudinally from extensive-discontinuous (50-90% areal permafrost coverage) in the north to sporadic-discontinuous (10-50%) in the south. Within this region, the Taiga Plains ecozone is comprised of a patchwork of mineral and organic terrain.



130 This study targets the peat plateau-collapse scar wetland complexes found in areas of high
peatland coverage (Wright et al. 2009; Helbig et al. 2016a). While temperature is the
predominant control on permafrost, the presence of near-surface organic materials can allow
permafrost to exist where mean annual air temperatures (MAATs) near, or even exceed 0°C, due
to the thermal offset between the ground surface and permafrost table created by insulating dry
135 peat soil layers (Vitt et al. 1994; Camill and Clark 1998). Dry (*i.e.* unsaturated) peat is a highly
effective thermal insulator, and for this reason, permafrost presence in peat plateau-wetland
complexes is largely restricted to peat plateaus (Zoltai & Tarnocai 1975; Hayashi et al. 2004;
Quinton et al. 2009). The areal coverage of permafrost in the discontinuous zone has
significantly decreased in recent decades due to increasing MAATs and has resulted in a shift
140 towards more wetland-dominated landscapes (Thie, 1974; Robinson and Moore, 2000; Wright et
al. 2009; Quinton et al., 2011; Olefeldt et al. 2016).

The discontinuous permafrost zone of the Taiga Plains ecozone covers 312,000 km² and
is here divided into the areas corresponding with extensive-discontinuous (151,000 km²) and
sporadic-discontinuous (161,000 km²) classifications (Brown et al., 2002; Figure 1). The region
145 is bounded by the Taiga Cordillera to the west and Taiga Shield to the east and is characterized
by a dry continental climate with short summers and long, cold winters with MAATs ranging
from -5.5°C to -1.5°C (Vincent et al. 2012). Much like the documented panarctic warming trend
(Overland et al., 2019), MAATs have increased across the Taiga Plains where the region has
experienced warming by as much as 2°C over the past 50 years (1970 – 2019) (Vincent et al.
150 2012). This is largely due to increases in average winter and spring temperatures of
approximately 3°C over the same time period (Vincent et al. 2012). Mean annual precipitation
has largely been consistent in this region over the past 50 years (Mekis & Vincent, 2011).



155

Figure 1: The Taiga Plains ecoregion with the discontinuous permafrost zones (coloured) defining the study region. The location of Scotty Creek Research Station (SCRS) is also indicated. Contains information licensed under the Open Government Licence – Canada.

2.1.1 Scotty Creek, NWT

The Scotty Creek Research Station (SCRS; 61.3°N, 121.3°W) has been the site of
160 extensive field-based studies over the past 20 years and provides an opportunity to use long-term
and detailed datasets that are uncommon in northern research (Quinton et al. 2019). The
trajectory of change proposed in this study is based upon observational data collected by the
SCRS and geospatial data across the broader study region. SCRS is located near the confluence
of the Mackenzie and Liard Rivers, and is approximately 50 km south of Fort Simpson in the



165 Northwest Territories (Figure 1). The MAAT (1970-2015) in Fort Simpson is -2.6°C , with a
mean annual precipitation (1970-2015) of 400 mm, of which mean annual snowfall accounts for
150 mm (Environment and Climate Change Canada 2019). Much like the broader Taiga Plains
region, temperatures in Fort Simpson have been steadily increasing, particularly during the
winter months (Vincent et al. 2015). Scotty Creek drains a 152 km^2 area dominated by peatlands
170 ranging in thickness between 2 and 8 m overlying a clay and silt rich glacial till (Quinton et al.,
2019). The peatland portion of the landscape is represented by peat plateau-collapse scar wetland
complexes, where permafrost predominantly occurs below the forested plateau features, while
the surrounding wetlands (specifically channel fens and collapse scar bogs) are devoid of
permafrost and are typically treeless (Hayashi et al. 2004; Quinton et al. 2009).

175 There is growing evidence that plateau-wetland complexes within peatland-dominated
environments are highly susceptible to shifts in the direction and magnitude of water and energy
fluxes in response to climatic changes (St. Jacques & Sauchyn 2009; Quinton et al. 2019). The
SCRS presents a unique opportunity to study warming-induced landcover changes to plateau-
wetland complexes in the Taiga Plains given the relatively long record of field and modelling
180 studies at this site, which have coincided with a period of drastic climate warming. Long-term
observations from field research and monitoring by the SCRS facilitates the examination of the
impacts of climate change on peat plateau and collapse scar wetland-dominated landscapes,
which are not only found extensively throughout northwestern Canada but also across the global
subarctic (Olefeldt et al. 2016).

185 **2.2 Geomatics Methods**

Geomatics methods were used to estimate the current distribution of peatlands, forest, and
permafrost across the study area. The discontinuous permafrost portion of the Taiga Plains



ecozone (depicted in Figure 1) was selected as the boundary for the regional scale geomatics work completed in this study. Multispectral Landsat 8 imagery (30 m resolution) was acquired across an area of over 300,000 km² totalling 70 Landsat scenes. Of these, 59 scenes were used to construct the base of the mosaic and 11 were used as secondary data to patch and minimize cloud cover. The 59 primary scenes were acquired in 2017 and 2018 while the 11 secondary scenes were acquired between 2013 and 2016 as data of suitable quality was unavailable during the preferred time period. Warm-season image acquisition was selected to prioritize snow-free scenes and to minimize seasonal variations in soil moisture that can also alter surface albedo particularly near wetland boundaries (Chasmer et al. 2010). As such, all 70 Landsat tiles were acquired in June, July, or August, rendering the images seasonally comparable and allowing for a more streamlined mosaicking process. A colour infrared mosaic (Landsat 8 bands 5, 4, 3 displayed as R, G, B) was created across the study region in ArcGIS (ESRI, Redlands, California) using a Lambert Conformal Conic projection. The mosaic dataset was colour balanced and the boundary was amended to the Taiga Plains ecozone including the delineations dividing the sporadic and extensive discontinuous zones (Brown et al. 2002).

To determine the current distribution of plateau-wetland complexes and related permafrost, the Landsat mosaic dataset was combined with two complementary products using the ArcGIS suite of programs. First, a saturated soils dataset (Natural Resources Canada 2017) was selected to isolate areas that were wetland-dominated and likely representative of the plateau-wetland complexes targeted in this study. Next, the Northern Circumpolar Soil Carbon Database (NCSCD) (Bolin Centre for Climate Research 2013) was selected to identify peatlands within the highlighted wetland-dominated areas. The two datasets were then masked to the Taiga Plains study region and combined in ArcGIS. The resultant product was mapped to display peatland terrain across the study region.



An unsupervised landcover classification was subsequently completed across the areas identified by the saturated soils and NCSCD datasets to identify and classify the landcovers within peat plateau-wetland complexes. The first iteration of the unsupervised classification (Iso Cluster classification approach) targeted 50-75 classes (72 created). The original 72 classes were then aggregated into 12 final classes within the peatland terrain outlined across the Taiga Plains study region. The final 12 aggregated classes include: coniferous (dense and sparse), mixed (dense and sparse), and broad leaf forests stands (dense and sparse), bog, fen, open water, bare ground, cloud, and cloud shadow. The results of this classification were used in combination with the map of peatland distribution in order to identify the forested landcovers within this broader terrain type. Forested peatlands are particularly indicative of landscape change in this region (Quinton et al. 2010; Baltzer et al. 2014; Chasmer & Hopkinson 2017) and as such, the proportion of coniferous forested area within the total peatland area was quantified across the region's latitudinal span. Proportional coniferous forested area was selected rather than total forested area to account for the observed spatial differences in peatland distribution across the Taiga Plains. For each degree of latitude, a bin was created for proportional forested area and the median was calculated alongside upper (*i.e.* 75th percentile) and lower (*i.e.* 25th percentile) quartiles. This data was plotted as a function of latitude across the study region. This generated a spatially distributed dataset of forest cover across the peatland-dominated regions of interest that was subsequently complemented by field data collected by the SCRS to guide the proposed conceptual model.

2.3 Field-based Methods

Intensive field studies first began at Scotty Creek in the 1990s with the goal of better understanding northern peatland landscapes (Quinton et al. 2019). A comprehensive archive of



ground-based energy and water measurements was used in this study to examine the temporal variation in landscape characteristics at Scotty Creek. These measurements helped to inform a conceptual model that simultaneously describe both the evolution of peat plateau-collapse scar wetland complexes subject to a warming climate and also the landscape transition from north-to-
240 south across the latitudinal and climatic gradient of this study. With each transitional stage of permafrost thaw-induced landcover change occurring in localized areas throughout the Scotty Creek basin and its location near the mid-latitude of the discontinuous permafrost zone, the conceptual model developed using SCRS data also intends to act as a microcosm of the broader landscape change occurring across the Taiga Plains.

245 Field research at Scotty Creek has improved the understanding of plateau-wetland complexes that not only dominate the headwaters of the Scotty Creek watershed but also much of the Taiga Plains ecoregion (Quinton et al. 2019). Collectively, these studies have contributed to establishing an understanding of the form and hydrological function of the major landcover types (*i.e.* permafrost plateau, collapse scar bog, and channel fen). These studies have also
250 demonstrated how these functions are changing with permafrost thaw (Quinton et al. 2019). In this study, three components of the hydrological cycle were selected to demonstrate this change: runoff, evapotranspiration, and storage. Precipitation data were also collected by the SCRS for use in the water balance portion of this study. Interannual precipitation data was collected with a Geonor precipitation gauge (Model T200B), which was installed in 2008. The Geonor data
255 include both rain and snow measurements logged at 30 minute intervals (Table 1). Despite no recorded changes in precipitation logged by the SCRS, in recent years Connon et al. (2014) and Haynes et al. (2018) have documented increases in runoff in the Scotty Creek watershed and adjacent watersheds with longer (~ 40 year) hydrometric records. It is suggested this could be attributed to increases in wetland connectivity due to permafrost thaw-induced landscape change.



260 Runoff (mm year^{-1}) between 1996 and 2012 was reported in Connon et al. (2014) and extended
to 2017 by Haynes et al. (2018), and is used in the runoff component of the conceptual model
presented here (Table 1).

265 Table 1: Annual precipitation (2008-2019), runoff (1996-2017), evapotranspiration
(2013-2016), and residual storage values are presented (mm year^{-1}) for two distinct
transitional landscape stages at Scotty Creek: a landscape dominated by forest and a
patchwork landscape of near-equal forest and treeless wetland landcovers. Both of these
landscapes represent transitional stages that Scotty Creek has undergone, where more
forest-dominated landscapes are more stable whereas increasing wetland presence can be
seen as an indicator of rapid permafrost thaw.

	FOREST > WETLAND	FOREST \approx WETLAND
PRECIPITATION	493	493
RUNOFF	149	215
EVAPOTRANSPIRATION	206	255
RESIDUAL STORAGE	138	23

270

Evapotranspiration has also been recently studied at the SCRS by Warren et al. (2018),
who reported evapotranspiration for forests, bogs, and the integrated landscape within the Scotty
Creek watershed between 2013 and 2016. Warren et al. (2018) described the variability in
evapotranspiration for these landcovers and quantified the minimal contribution of
275 evapotranspiration in forest-dominated landscapes due to the poor transpiration of black spruce
vegetation. Warren et al. (2018) reported daily evapotranspiration values (mm day^{-1}), which were
then converted to annual evapotranspiration (mm year^{-1}) for this study. These annual values were
used in the evapotranspiration component of the conceptual model in this study (Table 1).
Storage was calculated as the residual of precipitation inputs and evapotranspiration and runoff
280 outputs for this conceptual model (Table 1). Annual runoff, evapotranspiration, and storage were
analyzed to determine the relative trends in the water balance that are likely to occur across the
proposed trajectory of change (assuming unchanging annual precipitation).

Imagery of the Scotty Creek basin was also utilized to quantify and plot the changing
landcover patterns across the proposed trajectory. The SCRS has acquired aerial photos from



285 1947, 1970, and 1977 alongside IKONOS satellite imagery from 2000 and Worldview satellite
imagery from 2010 and 2018. The three historical aerial photographs (0.5-1.2 m resolution) and
IKONOS imagery (4 m resolution) were classified and results were presented in Quinton et al.
(2010). Landcover classifications were similarly completed on 2010 Worldview imagery by
Carpino et al. (2018). Additionally, Disher (2020) classified the Scotty Creek basin using the
290 most recently acquired 2018 Worldview imagery to update the record of permafrost thaw-
induced landcover change. The total area of each landcover (*i.e.* forested plateau, collapse scar
wetland, and afforested wetland) as a proportion of the total area was calculated for both the
historical air photos and more modern satellite imagery at each site. The plotted changes to
landcover proportions between 1947 and 2018 at Scotty Creek were evaluated against the
295 conceptual model.

Changes to water (*e.g.* Connon et al. 2014; Haynes et al. 2018; Warren et al. 2018) and
landcover (*e.g.* Quinton et al. 2010; Baltzer et al. 2014; Carpino et al. 2018; Disher 2020) due to
climate warming and permafrost thaw have been well documented in previous work by the
SCRS. However, to determine changes to the energy balance across the proposed trajectory, four
300 meteorological stations at Scotty Creek were selected for use in this study. The first
meteorological station used was installed in a collapse scar wetland in 2004 (hereafter wetland
station) followed by a second station on a densely forested peat plateau in 2007 (hereafter dense
plateau station). Two additional stations located on forested plateaus were also selected to
represent the variety of canopy densities that are increasingly apparent with permafrost thaw-
305 included landcover change (Chasmer & Hopkinson 2017; Haynes et al. under review). These
stations were installed on a sparsely forested peat plateau in 2015 (hereafter sparse plateau
station) and a forested plateau with an intermediate canopy in 2014 (hereafter intermediate
plateau station).



Four component radiation data were collected at the dense plateau, sparse plateau, and
310 wetland meteorological stations, while only shortwave radiation was collected at the intermediate
plateau station. Haynes et al. (2019) thoroughly summarize the instrumentation within the Scotty
Creek basin. All radiation data were collected at 30 minute intervals and compiled into daily
averages. The daily average radiation data was used to calculate annual averages across each
station's record length. These annual averages were plotted alongside the proposed trajectory
315 according to the transitional stage that most appropriately matched the landcover represented by
each meteorological station. While using four meteorological stations (three of which represent
plateau landcovers), accounts for some of the variability present across the landscape, there is
also strong spatial and temporal variability in subcanopy shortwave and longwave radiation
(Webster et al. 2016). To address this more localized subcanopy variability, the daily average
320 four component radiation data from each station were compared on a monthly time step. The
monthly averages were calculated and compared across the landcovers represented by each of
the four meteorological stations using a one-way analysis of variance (ANOVA) with Tukey
post-hoc test ($\alpha = 0.05$).

Data compiled from the SCRS were used to inform the conceptual model of landscape
325 transition proposed in this study. The conceptual model presents both the landcover changes
anticipated as an environment experiences permafrost thaw as well as the associated changes to
water and energy. Illustrations were created to represent each stage in the proposed trajectory of
landscape transition. Complementary imagery was collected using a Remotely Piloted Aircraft
System (RPAS) at Scotty Creek to represent how each of these illustrated trajectory stages
330 manifests on the landscape in a peat plateau and collapse scar wetland-dominated environment.
The RPAS imagery (0.5 m resolution) was collected in the summer of 2018 using an eBee Plus
equipped with a senseFly SODA 3D mapping camera and all image processing was completed in

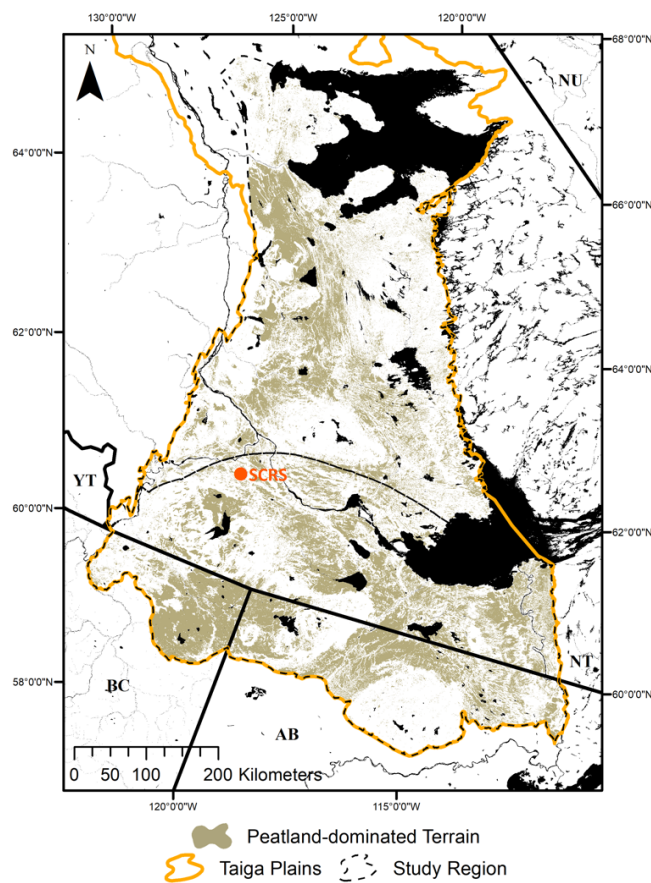


Pix4DMapper. The changes in energy and water balances identified in literature and data analysis for this study were calculated according to the landcover and transitional stage
335 represented by these data. The changes to landcover at Scotty Creek were also presented as a summary plot within the conceptual model to illustrate the observed and recorded changes over time. As each of the stages of landscape transition proposed in the conceptual model are also observed at Scotty Creek, ongoing shifts in landcover and the associated hydrometeorological changes can be extrapolated to other peat plateau-collapse scar wetland sites similar to Scotty
340 Creek.

3. Results and Discussion

3.1 Peatland and Permafrost Distribution

The geomatics methods applied in this study indicate that the peatland-dominated terrain often supporting permafrost is distributed across the Taiga Plains (Figure 2). Expectedly, large
345 peatland clusters are located in lowland areas with high histel soil percentages. In the extensive-discontinuous permafrost zone, peatlands are clustered to the west, nearest to the Mackenzie River, and are largely absent from the eastern study region in the area bounded by Great Bear Lake to the north and the Taiga Shield to the east. In the sporadic-discontinuous zone, the distribution of these peatland clusters is more longitudinally dispersed. We estimate that
350 approximately 35% of the discontinuous permafrost zone within the Taiga Plains ecozone is composed of landscapes with high peatland coverage.

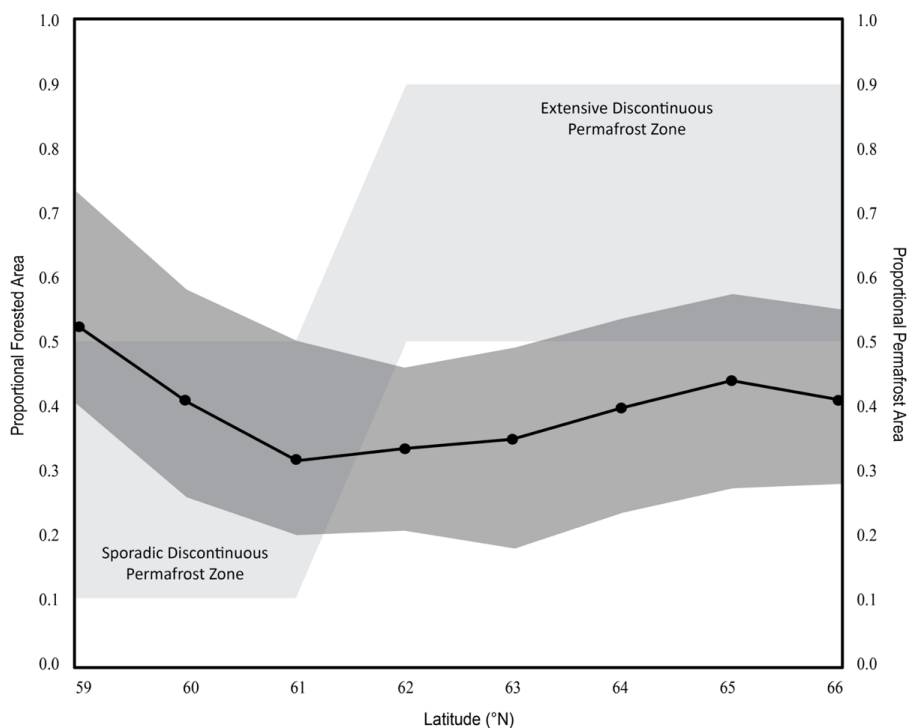


355 Figure 2: Predicted distribution of peatland-dominated terrain in the discontinuous permafrost zone of the Taiga Plains. Peatland-dominated terrain was determined using a saturated soils dataset (Natural Resources Canada 2017), the NCSCD (Bolin Centre for Climate Research 2013), and Landsat 8 Data from the United States Geological Survey. Contains information licensed under the Open Government Licence – Canada.

As changes to forested landcovers have been used as an indicator of broader landscape
360 change in this region (Baltzer et al. 2014; Chasmer & Hopkinson 2017), forested peatlands,
including forested peat plateaus in plateau-wetland complexes and forested permafrost-free
wetlands were plotted as a function of latitude (Figure 3). A latitudinal trend in landcover
percentage is apparent within the identified areas of high peatland coverage. Along the boundary



between the extensive-discontinuous and sporadic-discontinuous permafrost zones in the centre
365 of the study region, wetland features, including collapse scar bogs, are most prevalent. Median
proportional forest cover reaches its minimum at $\sim 33\%$ within the 61°N bin, the latitude at
which SCRS is also located. The proportion of forested peatlands remains relatively low across
the transitional zone between sporadic and extensive discontinuous permafrost as median forest
cover does not exceed 34% between 61 and 62°N . As collapse scar wetlands appear to be
370 widespread in this area, permafrost thaw and increased inundation and waterlogging of
previously dry peat plateaus may be most drastic at the mid-latitudes of the study region (Islam
& Macdonald 2004; Iwata et al. 2012). However, in both the extensive discontinuous permafrost
zone to the north and the sporadic discontinuous permafrost zone to the south, relative increases
in proportional forested peatland area are observed.



375

Figure 3: Median forested peatland area proportional to total peatland area plotted as a function of latitude. The extent of the band represents the range of proportional forested peatland area between the 25th percentile and 75th percentile. Permafrost extent as a proportion of total area is also plotted across the same latitudinal range in light gray.

380

In the extensive-discontinuous permafrost zone (63 – 66°N), the median proportion of forested peatlands ranges from ~ 35 – 45% , indicating that forested peatlands, including the peat plateaus that support permafrost in plateau-wetland complexes, are more intact than across the transitional boundary zone. This has been explained through lower MAATs and the insulating properties of the dry peat that dominates the near-surface of these plateau-wetland complexes (Zoltai & Tarnocai 1975; Hayashi et al. 2004). The sporadic-discontinuous permafrost zone consists of ~ 50% (59 – 60°N) forest cover in peatlands, including the greatest median proportional forested area at ~ 52%. Here, afforestation of permafrost-free peatlands appears to be responsible for some of the forested area along the southern boundary of the study region,

385



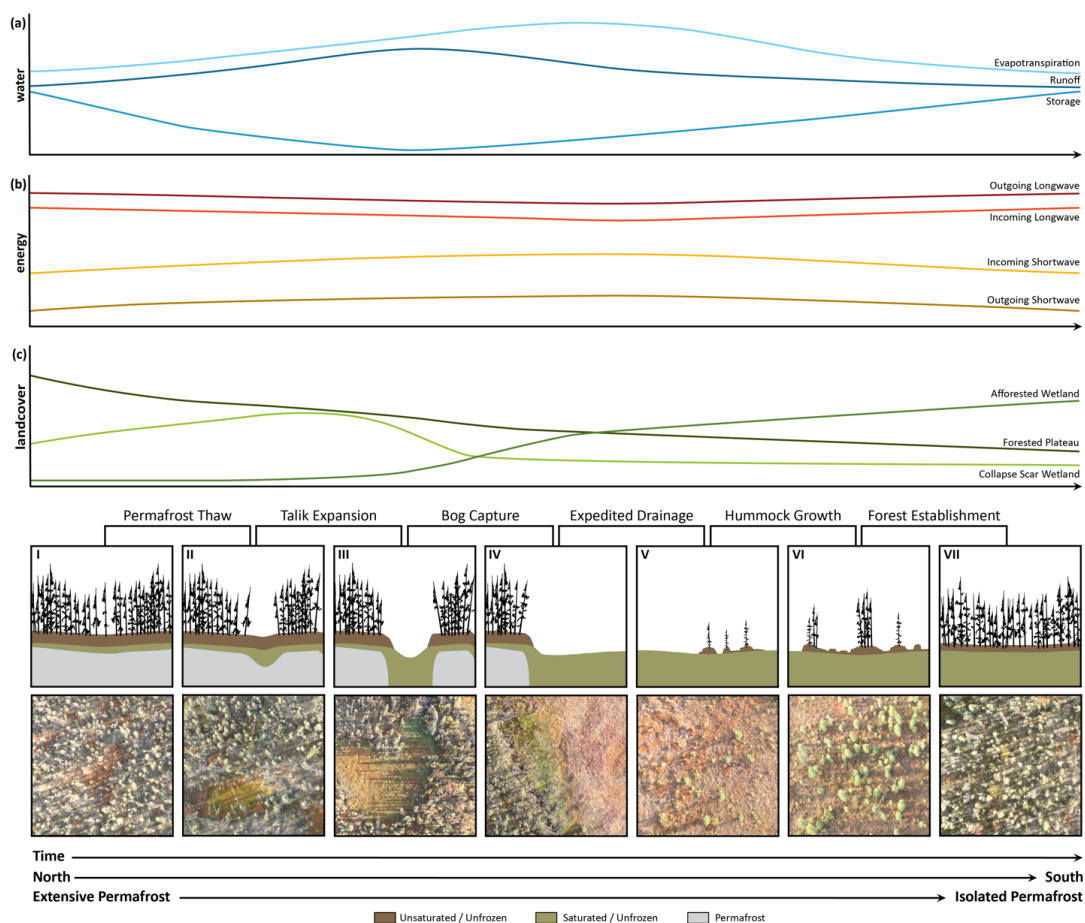
390 particularly in the areas of northern British Columbia and northern Alberta; a pattern also
observed in Carpino et al. (2018), but first reported by Zoltai (1993). This suggests that a large
portion of permafrost has already been lost from these environments as peatland dewatering
lowers the water table (Ketteridge et al. 2013; Haynes et al. 2018), allowing for forest cover to
return to newly unsaturated areas (Zoltai 1993; Camill 1999).

395 **3.2 Plateau-Wetland Complex Landscape Trajectory**

The evolution of peat plateau-collapse scar wetland complexes over time can be
represented by seven phases: (I) Forested permafrost plateaus; (II) Forested permafrost plateaus
with small, isolated collapse scar wetlands; (III) Forested permafrost plateaus with larger,
interconnected wetlands; (IV) Wetland complexes with small plateau islands; (V) Wetland
400 complexes with small-scale hummock development and tree establishment; (VI) Hummock
growth with forest establishment; and (VII) Afforested wetlands (Figure 4). A sequence of
hydrological processes and energetic mechanisms occurs to initiate landscape change and drive
the landscape along the proposed spectrum of transition. As permafrost thaw commences, a
landscape dominated by forested plateaus and underlain by permafrost (Figure 4I) transitions to
405 one with small, suprapermfrost taliks (Connon et al. 2018) and isolated collapse scar bogs begin
to emerge (Figure 4II; Quinton et al. 2011). As permafrost thaw and talik development
continues, the previously isolated collapse scars expand (Figure 4III; Devoie et al. 2019) and
become interconnected with surrounding wetlands (Connon et al. 2015). As permafrost thaw
continues, wetlands proliferate and become increasingly connected, creating a landscape
410 dominated by widespread wetland complexes with only isolated plateau islands (Figure 4IV;
Baltzer et al. 2014; Chasmer & Hopkinson 2017).



The predominance of wetland features on the landscape is also coupled with increased and expedited drainage (Connon et al. 2014; Haynes et al. 2018). Over time, small-scale hummock microtopography emerges towards the centre of these draining wetlands (Figure 4V; 415 Haynes et al. under review) and black spruce trees begin to re-establish on these features (Figure 4VI; Iversen et al. 2018; Dymond et al. 2019). Continued hummock growth allows for afforestation to continue (Eppinga et al. 2007; Iversen et al. 2018) until the landscape returns to a forest-dominated landscape that appears similar to the original stage in as little as 40 years (Figure 4VII; Carpino et al. 2018). However, the widespread permafrost aggradation predicted 420 by Zoltai (1993) and Camill (1999) is unlikely to occur under the region's current and warming climatic conditions. Instead, small patches of isolated frozen ground may be able to re-establish under the new black spruce canopy on an interannual basis, but is unlikely to exist at a landscape scale or to persist on a long temporal scale.



425 Figure 4: (Bottom) Proposed conceptual model of landscape trajectory including a space-
 430 for-time substitution for changes to both permafrost and landcover. Conceptual diagrams
 are presented to illustrate landscape change with the support of RPAS imagery collected
 at the SCRS. The conceptual model is presented alongside the processes that initiate the
 trajectory's progression. (a) Relative changes to local water balances of measured SCRS
 435 runoff, evapotranspiration and residual storage with unchanging precipitation are
 summarized and presented over the trajectory of landscape change based on the
 proportion of forested vs. wetland area. (b) Relative changes to local energy balances
 are presented using data collected from meteorological stations installed at Scotty Creek.
 (c) Changes to relative landcover proportions are presented using historical aerial
 photographs and recent acquisitions of satellite imagery over the Scotty Creek basin.



This transition not only represents the dominant trajectory of change observed over recent decades in the Scotty Creek basin (Quinton 2019), but also corresponds with the north-south climatic transition of peatland-dominated plateau-wetland complexes spanning northwestern Canada's zone of discontinuous permafrost. This spans the extensive permafrost found beneath treed peat plateaus in the north, to patchwork or even wetland-dominated landscapes at more moderate latitudes, and finally to more widespread permafrost-free environments at the southern extent of the Taiga Plains. Each of these stages, and the transitional steps between them, can also be observed at smaller scales at local sites including Scotty Creek, which is located on the boundary between the sporadic-discontinuous and extensive-discontinuous zones. The Scotty Creek Research station is in phase III-IV, with localized conditions that correspond to the range of other phases. This exemplifies the concurrent nature of the phases along the spectrum of landscape transition.

3.2.1 Landcover Trajectory

Changes to the relative proportions of the three main landcovers represented across the trajectory (Figure 4c) (forest plateau, collapse scar wetland, and afforested wetland) have been observed at the landscape-scale with remotely-sensed imagery. At Scotty Creek, the early portions of the trajectory (*i.e.* stages I, II) represent the changes observed between 1947 and 2000 as the landscape transitioned from predominantly forested and underlain by permafrost to one defined by a forest-wetland patchwork and degrading permafrost bodies (Quinton et al. 2010). This ~ 50 year period shows a change in proportional landcover as forested areas move from covering approximately 70% of Scotty Creek to approximately 50% (Quinton et al. 2010; Baltzer et al. 2014). This forest loss directly corresponds with wetland expansion at the expense of permafrost as treeless wetland features (both collapse scar bogs and channel fens) shift from approximately 30% of the landcover to approximately 50% over the same time period (Quinton



et al. 2010). As of 2018, the headwaters of the Scotty Creek basin were comprised of approximately 40% forested permafrost plateau, 45% treeless wetland (13% collapse scar wetland and 32% channel fen), and 13% afforested wetland (Disher 2020). These results indicate
465 that the proportional area of peat plateau, and thus permafrost terrain, has continued to decline since previous analyses (Quinton et al. 2010; Baltzer et al. 2014; Connon et al. 2014; Carpino et al. 2018). While permafrost thaw-induced forest loss continues rapidly at Scotty Creek, forest re-establishment is also occurring in the form of afforested wetlands (Disher 2020). As such, these results are also indicative of the fact that the transition from one stage of the trajectory to the next
470 is not instantaneous and can occur to varying degrees within a local site such as Scotty Creek.

Between 1970 and 2010 the Scotty Creek watershed had lost approximately 12% of its forested permafrost plateau area (Carpino et al. 2018). Landscape wide, the Scotty Creek basin is, as of 2018, most closely represented by the transition from stage III to IV, where forest and permafrost loss continue to dominate, but forest re-establishment is becoming increasingly
475 apparent as the wetlands begin to drain more readily. The transition of forest to wetland is expected to continue until the later stages of the trajectory, when increases in afforestation will be observed, yielding decreases in the proportional area of both forested plateaus and collapse scar wetlands (Ketteridge et al. 2013; Chasmer & Hopkinson 2017; Warren et al. 2018). While Scotty Creek and many similar sites continue to undergo active transition from plateau to
480 wetland, afforested wetlands are appearing across the site and may have previously been misclassified as forested plateau area (Disher 2020). The emergence of afforested wetland landcovers has previously been documented in sites along the southern margin of sporadic discontinuous permafrost, particularly in northeastern British Columbia (Carpino et al. 2018). These sites experienced an even more accelerated transition from forest to wetland and lost close
485 to 17% of forested plateau area over the same 1970-2010 period (Carpino et al. 2018). However,



these sites also demonstrated an almost 10% gain in afforested wetland over the same 40-year time period (Carpino et al. 2018).

In addition to establishing the predominant direction of change across the region, the proposed landscape trajectory also corresponds to a succession of plant communities related to each stage's degree of wetness. Early stages of landscape transition are characterized by the presence of relatively undisturbed black spruce tree cover (Figure 4I). As permafrost thaw progresses, changes to the *Sphagnum*-dominated communities within collapse scar features are an indicator of vegetation succession, demonstrating a wetness-based zonation (Zoltai 1993). Specifically, aquatic *Sphagnum* species, notably *S. riparium*, occupy the inundated margins between actively thawing permafrost plateaus and developing collapse scar bogs (Garon-Labrecque et al. 2015; Pelletier et al. 2017). Young and expanding collapse scar bogs are most easily identified by the distinct bright green colour of *S. riparium* as seen in high-resolution RPAS imagery (Figure 4II, III, IV; Gibson et al. 2018; Haynes et al. under review) but their margins may also be identified by bare peat banks or moats of water directly along the permafrost plateau edge (Zoltai 1993). As collapse scars expand, lawn species, such as *S. angustifolium*, and hummock species, such as *S. fuscum*, emerge, particularly towards the bog centre (Zoltai 1993; Camill 1999; Pelletier et al. 2017). Hummock species are especially dominant towards the centre of collapse scars, establishing themselves on top of continuous and sufficiently compacted peat above the water table (Camill 1999; Loisel & Yu 2013). Much like *S. riparium*, *S. fuscum* is easily identifiable in high-resolution imagery by colour. The distinct russet colour of *S. fuscum*, (Figure 4V) alongside the textured hummock microtopography apparent in high-resolution digital terrain models, provides evidence to aid in classifications (Haynes et al. under review). The abundance of relatively dense *S. fuscum* hummocks allows for the re-establishment of black spruce (Liefers & Rothwell 1987), first on isolated hummocks



510 (Figure 4VI) but eventually leading to widespread afforestation (Figure 4VII; Camill 2000;
Ketteridge et al. 2013). Ultimately, these successional changes to *Sphagnum* communities
provide clear support to the proposed trajectory, progressing from aquatic-to-lawn-to-hummock
dominated collapse scars before these features are open to forest re-establishment (Iversen et al.
2018; Dymond et al. 2019).

515 3.2.2 Energy Trajectory

The Scotty Creek watershed serves as a microcosm of the transition observed across the
Taiga Plains with respect to their water and energy budgets. While energy budgets measured at
Scotty Creek are expectedly similar across the landscape, some general trends are present (Figure
4b). Annual shortwave radiation, both incoming and outgoing, peaks over the middle stages of
520 the trajectory (IV, V); where treeless collapse scar bogs are the dominant landcover. Annual
shortwave radiation, both incoming and outgoing is comparatively lower in forested stages of the
trajectory. Specifically, lowest annual shortwave contributions (both incoming and outgoing) are
observed at the dense plateau station (I). Both incoming and outgoing annual longwave radiation
are greatest in the more densely forested landscapes present at the beginning (I, II) and end
525 stages of the trajectory (VI, VII) and lowest in the wetland landscapes that dominate the middle
stages (IV, V).

Given the spatial and temporal variability of four component radiation data, averages at
each of the four stations representing the different tree canopy densities observed along the
spectrum of landscape change were also compared (Figure 5). Differences between stations were
530 assessed for statistical significance by one-way ANOVA using monthly data over the length of
record available at each station. There were statistically significant differences between stations
for incoming shortwave (Figure 5a), outgoing shortwave (Figure 5b), and incoming longwave
(Figure 5c), while outgoing longwave showed no statistical differences between stations (Figure



5d). To determine significant differences between each of the landscape types represented by the
535 four meteorological stations, a Tukey post-hoc test was used for each of the four radiation
components.

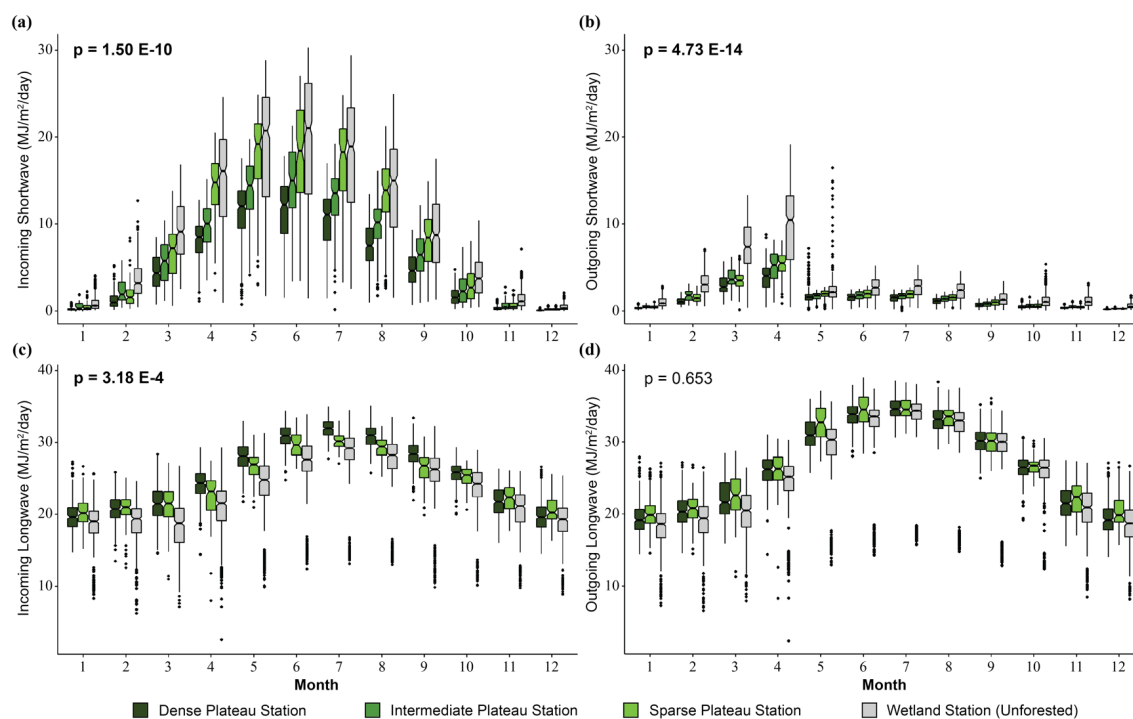


Figure 5: Four component radiation plots (MJ/m²/day) displaying (a) incoming shortwave, (b) outgoing shortwave, (c) incoming longwave, and (d) outgoing longwave across four meteorological stations. Each station represents a distinct landcover: dense plateau (2007-2019), intermediate plateau (2014-2019), sparse plateau (2015-2019), and tree-free wetland (2004-2019). The four meteorological stations are presented as notched box and whisker plots across 12 months where the boxes represent the 25th and 75th percentile, while the whiskers represent the range of the data. The notches on each box indicate the confidence interval ($\alpha = 0.05$) around the mean while the statistical differences between meteorological stations have been presented in the upper left of each plot as determined by one-way ANOVA. Significant p values have been highlighted with bold text.

540



545 Shortwave radiation, both incoming and outgoing, showed significant differences
between landcovers. However, a Tukey post-hoc test revealed that there was variability between
the two shortwave components for which groups specifically showed these significant
differences. As the four meteorological stations fall along a gradient of forest density from a
completely unforested wetland to a densely forested plateau, no significant differences in
550 incoming shortwave radiation were ever found between stations only one rank apart on that
gradient. As such, measurements indicate average monthly incoming shortwave radiation is
significantly greater at the wetland compared to both the intermediate plateau ($p = 2.82 \times 10^{-4}$)
and the dense plateau ($p = 1.055 \times 10^{-10}$), while no significant difference exists between wetland
and the sparse plateau. On the other end of the gradient, the dense plateau receives significantly
555 less incoming shortwave radiation than both the wetland ($p = 1.055 \times 10^{-10}$) and the sparse
plateau ($p = 0.036$), but this station is not significantly different from the intermediate plateau.
Outgoing shortwave radiation follows a slightly different pattern as no significant differences
exist between any of the forested plateau stations but all are significantly different from the
wetland. Specifically, outgoing shortwave radiation recorded at the wetland station is
560 significantly greater than the sparse plateau ($p = 4.5 \times 10^{-5}$), intermediate plateau ($p = 2.0 \times 10^{-5}$),
and dense plateau stations ($p = 4.814 \times 10^{-13}$). The differences between the wetland station and
the forested plateau stations also become progressively more significant with increasing tree
density. There was a statistically significant difference between the three stations (intermediate
plateau omitted due to lack of measurements) for incoming longwave radiation, while no
565 statistically significant differences were observed in the outgoing longwave radiation component.
The only significant difference in incoming longwave was observed between the wetland and



dense plateau ($p = 2.26 \times 10^{-4}$). No significant differences exist between the sparse plateau and the wetland or dense plateau.

The radiation data plotted follows the patterns that would be expected at a subarctic site
570 such as Scotty Creek, where drastic decreases in available energy are observed in winter months
(Figure 5). At sites like Scotty Creek, where a forest-wetland patchwork is present, the observed
differences in radiation between the landcovers represented by each meteorological station can
also be amplified by temporal variability. Differing surface properties, particularly albedo, at
each landcover type can alter the impact of shortwave radiation on the landscape. Wetland
575 albedo has been observed to be consistently higher than forest albedo at Scotty Creek as black
spruce forests cover the more reflective ground cover (*e.g.* mosses, lichen, deciduous shrubs,
etc.) (Helbig et al. 2016b). However, the differences in albedo are further exaggerated when
snowcover is present as black spruce forests also mask the highly reflective snowcover (Helbig
et al. 2016b). As incoming shortwave radiation increases towards the end of winter in the period
580 leading up to snowmelt, the impact of albedo on outgoing shortwave radiation is particularly
prominent. This is evident as outgoing shortwave radiation at the wetland station increases ahead
of the forested stations during late winter and then peaks in the spring due to the impact of
albedo at the tree-free wetland site (Figure 5b). At sites such as Scotty Creek, where permafrost
thaw-induced landcover change is observed as a shift from forest to wetland, an increase in
585 landscape albedo has been observed (Helbig et al. 2016b). This could lead to a regional cooling
effect across the southern Taiga Plains, particularly during winter months when differences in
albedo are greatest between forest and wetland landcovers (Helbig et al. 2016b). A warming
effect was observed during summer months in areas experiencing active forest loss as a thinning



forest increased the ground heat flux, and is consistent with the ongoing permafrost thaw
590 observed on forested plateaus at Scotty Creek (Helbig et al. 2016b).

In permafrost terrains, the flux of energy is closely coupled with both changes to
permafrost thaw rates (and therefore changes to landcover) as well as changes to runoff (Quinton
et al 1999). Canopy thinning due to permafrost thaw or other disturbances such as fire or seismic
exploration increases the radiation at the ground surface. This spatially heterogenous increase in
595 incoming radiant energy may be responsible for areas of accelerated permafrost thaw, resulting
in topographic variation across the frost table. This heterogeneity is suggested as the mechanism
driving the transition from stage I to II in the trajectory (Quinton et al. 2019). The topographic
variability in frost table results in preferential water storage in local depressions, increasing the
thermal conductivity and resulting in increased thaw (Quinton et al. 2019). This positive
600 feedback leads to the formation of depressions both at the ground surface and at the frost table,
altering local runoff pathways and increasing depressional storage (Wright et al. 2009; Quinton
et al. 2009). This positive feedback mechanism is furthered as increased surface wetness
accelerates canopy loss due to waterlogging and therefore increases both the thermal and
radiative energy received at the ground's surface. This feedback is present in the initial stages of
605 the trajectory, and is often associated with talik formation and expansion into collapse scars due
to localized permafrost loss (Chasmer & Hopkinson 2017; Connon et al. 2018).

3.2.3 Water Trajectory

At peatland-dominated sites such as Scotty Creek, changes to energy can act as a driver
of permafrost thaw-induced landcover change and are also closely coupled to changes in water
610 and runoff regimes. Therefore, as the trajectory progresses through the proposed stages, the
relative influence of the processes governing the hydrology of the landscape changes



dynamically (Figure 4a). The early stages (I, II) of the proposed successional trajectory are dominated by hydrologically isolated wetlands, where storage is maximized and outflow from the basin is limited to primary runoff from plateau features into nearby fens (Connon et al. 2014; 615 Quinton et al. 2003). Water arriving directly into one of the isolated, but rapidly expanding collapse scar wetlands will be stored as there is no direct flow path to the channel fen (Quinton et al. 2019). The contributions of evapotranspiration during the forest-dominated stages are similarly minor due to the limited transpirative ability of black spruce on organic soils (Warren et al. 2018). Even when forest is the predominant landcover, understory vegetation is the 620 principal contributor to evapotranspiration (Chasmer et al. 2011).

As the environment becomes more wetland dominated, runoff and storage diverge. By stage III, where wetlands are interconnected and rapidly expanding, storage reaches its minimum while runoff is maximized (Figure 4a). At this point in the trajectory, elevated runoff is due to the introduction of new runoff pathways (Connon et al. 2014), and from the drainage of water 625 previously stored in isolated wetlands (Haynes et al. 2018). Specifically, runoff is amplified by enhancing the runoff contributing area through connected and cascading wetlands, which are also responsible for the reduction in storage (Connon et al. 2015; Haynes et al. 2018). A decrease in runoff then follows as plateau loss continues to accelerate, eliminating transient contributions from interior collapse scar wetlands, increasing the basin storage and reducing the impact of 630 cascading wetlands (Quinton et al. 2019). At this point in the trajectory, the impact of storage and runoff on the overall water balance diminishes as evapotranspiration increases and eventually reaches its maximum. In the trajectory stages where wetland is the predominant landcover (IV, V), the evapotranspiration term peaks due to evaporation from standing water and exposed moss groundcover (Warren et al. 2018).



635 Finally, the advanced stages of the trajectory (VI, VII) correspond with continued
decreases in runoff, as well as decreases in evapotranspiration. Peatland dewatering acts as the
initial mechanism for the development of hummock microtopography and tree re-establishment
(Ketteridge et al. 2013; Chasmer & Hopkinson 2017). The afforested wetland landcover
proposed as the final stage in the trajectory has only recently been defined and studied at Scotty
640 Creek (Haynes et al. under review; Disher 2020) and as such, evapotranspiration, storage and
runoff measurements that are specific to afforested wetlands do not presently exist at the site.
Soil moisture across the afforested wetland landcover has been observed to be intermediate
between that of plateaus and collapse scar bogs (Haynes et al. under review). It is likely that
many of the thermal and hydrological characteristics of afforested wetlands would fall between
645 collapse scar bogs and forested plateau features as they are treed but permafrost-free. This would
likely result in similar evapotranspiration relationships to the forested permafrost plateaus that
dominate the early stages despite being permafrost-free. Storage and runoff may however
increase from the original forest-dominated landscape to a mid-level between plateau and
wetland values due to the lack of underlying permafrost and lower elevation.

650 Afforested wetland features have not been studied to the same degree as peat plateaus or
collapse scar wetlands and in some cases have been misclassified as either feature in the past
(Haynes et al. under review). Data that are specific to these features are lacking in comparison to
better-documented landforms even at sites such as Scotty Creek where intensive field studies are
ongoing. Further examination is warranted into the hydrology and energy dynamics at these
655 sites, particularly if afforestation represents an end-stage in the trajectory of peat plateau-collapse
scar wetland complexes. The impacts of increasingly widespread afforested wetlands on basin
runoff should be investigated as well as further work to confirm whether evapotranspiration for



this landcover is intermediary much like soil moisture appears to be (Haynes et al. under review).
Furthermore, the persistence and permanence of afforested wetland landcovers has not been
660 documented. Exploring canopy or stand properties such as age, health, and productivity across
these features may provide insight and assist in further defining the role of afforested wetlands in
the trajectory of plateau-wetland complexes.

4. Conclusions

The discontinuous permafrost zone of the Taiga Plains exemplifies a landscape in
665 transition. Coupling a broad-scale mapping initiative with the detail of site-specific data
collected at the SCRS emphasizes the close dependence of landcover on climate by way of local
energy and water budgets. Small changes to climate or tree cover can initiate permafrost thaw
and trigger a series of positive feedbacks related to energy, water and vegetation communities,
leading directly to changes across the landscape. The proposed conceptual model of landscape
670 evolution summarized in Figure 4 describes the transitions occurring across the Taiga Plains in
peat plateau-collapse scar wetland complexes like Scotty Creek. The evolution model is strongly
supported via both direct observations and synthesis of the literature and describes the shifts that
occur in energy and water budgets as the landscape transitions from forest underlain by
permafrost to permafrost-free afforested wetlands. We identify the likely region of applicability
675 of this conceptual model across a large region of the Canadian north. We also establish the
regional pattern of change across these environments and given the latitudinal gradient is a
suitable space-for-time proxy, project their future trajectory by combining long-term field
observations with analyses of contemporary and historical imagery. It is proposed that, while
permafrost thaw-induced landcover changes have previously been dominated by a transition
680 from forest to wetland, this transition is not permanent and forested landcovers are likely to



return over time, although not likely underlain by permafrost. This research improves our understanding of how changes to permafrost distribution and ongoing permafrost thaw may impact peatland-dominated environments and are of relevance to other peatland-rich permafrost environments across the circumpolar north.

685 **5. Acknowledgements**

We gratefully acknowledge the support of the Dehcho First Nations, in particular, the Liidlii Kue First Nation and Jean Marie River First Nation. We also thank these communities for their long-standing support of the Scotty Creek Research Station. This work was funded by ArcticNet through their support of the Dehcho Collaborative on Permafrost (DCoP), and by the
690 Natural Sciences and Engineering Research Council of Canada (NSERC). We also acknowledge the Canada Foundation for Innovation (CFI) for providing funding for infrastructure critical to this study.

6. Data Availability

The data used in this paper are in the process of being catalogued for open access in the Wilfrid
695 Laurier University (WLU) Data Repository, which is fully in compliance with all FAIR guidelines. While these data are being catalogued, the datasets used in this study are available upon request by contacting the corresponding author.

7. Author Contributions

All authors contributed to the development of the research question and the methodological
700 approach used in this study. OC performed the analyses and wrote the manuscript with input and editorial contributions from KH, RC, JC, ÉD and WQ.



8. Competing Interests

The authors declare that they have no conflict of interest.

9. References

- 705 Baltzer, J., Veness, T., Chasmer, L., Sniderhan, A., & Quinton, W. (2014). Forests on thawing
permafrost: Fragmentation, edge effects, and net forest loss. *Global Change Biology*,
20(3), 824-834. DOI: 10.1111/gcb.12349
- Beilman D.W. & Robinson S.D. (2003). Peatland permafrost thaw and landcover type along a
climate gradient. Proceedings of the Eighth International Conference on Permafrost, vol.
710 1. Phillips M., Springman S.M., & Arenson L.U., Eds. Balkema, Zurich, pp 61–65.
- Biskaborn, B.K., Smith, S.L., Noetzli, J. *et al.* (2019). Permafrost is warming at a global
scale. *Nature Communications*, 10(264). doi.org/10.1038/s41467-018-08240-4
- Box, J.E., Colgan, W.T., Christensen, T.R., Schmidt, N.M., Lund, M., Parmentier, F.W., Brown,
R., Bhatt, U.S., Euskirchen, E.S., Romanovsky, V.E., Walsh, J.E., Overland, J.E., Wang,
715 M., Corell, R.W., Meier, W.N., Wouters, B., Mernild, S., Mård, J., Pawlak, J. & Olsen,
M.S. (2019). Key indicators of arctic climate change: 1971-2017. *Environmental
Research Letters*, 14, 045010. doi.org/10.1088/1748-9326/aafc1b
- Brown, J., O. Ferrians, J. A. Heginbottom, and E. Melnikov. (2002). Circum-Arctic Map of
Permafrost and Ground-Ice Conditions, Version 2. Permaice subset used. Boulder,
720 Colorado USA. NSIDC: National Snow and Ice Data Center. Date accessed: Jan. 2020.
- Camill, P. (1999). Peat accumulation and succession following permafrost thaw in the boreal
peatlands of Manitoba, Canada. *Ecoscience*, 6(4), 592-602.
- Camill, P. (2000). How much do local factors matter for predicting transient ecosystem
dynamics? Suggestions from permafrost formation in boreal peatlands. *Global Change
725 Biology*, 6, 169-182. doi.org/10.1046/j.1365-2486.2000.00293.x
- Camill, P. & J. S. Clark, 1998. Climate change disequilibrium of boreal permafrost peatlands
caused by local processes. *American Naturalist*, 151, 207-222. DOI: 10.1086/286112
- Carpino, O.A., Berg, A.A., Quinton, W.L., & Adams, J.R. (2018). Climate change and
permafrost thaw-induced boreal forest loss in northwestern Canada. *Environmental
730 Research Letters*, 13(8). doi.org/10.1088/1748-9326/aad74e
- Chasmer, L. & Hopkinson, C. (2017). Threshold loss of discontinuous permafrost and landscape
evolution. *Global Change Biology*, 23, 2672-2686.
- Chasmer, L., Hopkinson, C. & Quinton, W. (2010). Quantifying errors in discontinuous
permafrost plateau change from optical data, Northwest Territories, Canada: 1947-2008.
735 *Canadian Journal of Remote Sensing*, 36(2), 211-223. DOI: 10.1111/gcb.13537
- Chasmer, L., Hopkinson, C., Veness, T., Quinton, W., & Baltzer, J. (2014). A decision-tree
classification for low-lying complex landcover types within the zone of discontinuous
permafrost, *Remote Sensing of Environment*, 143, 73–84.
doi.org/10.1016/j.rse.2013.12.016



- 740 Chasmer, L., Quinton, W., Hopkinson, C., Petrone, R., & Whittington, P. (2011). Vegetation Canopy and Radiation Controls on Permafrost Plateau Evolution within the Discontinuous Permafrost Zone, Northwest Territories, Canada. *Permafrost and Periglacial Processes*, 22(3). doi.org/10.1002/ppp.724
- 745 Cohen, J., Screen, J. A., Furtado, J. C., Barlow, M., Whittleston, D., Coumou, D., Francis, J., Dethloff, K., Entekhabi, D., Overland, J., & Jones, J. (2014). Recent Arctic amplification and extreme mid-latitude weather, *Nature Geoscience*. doi.org/10.1038/ngeo2234
- Connon, R., Devoie, É., Hayashi, M., Veness, T., & Quinton, W. (2018). The influence of shallow taliks on permafrost thaw and active layer dynamics in subarctic Canada. *Journal of Geophysical Research: Earth Surface*, 123, 281–297. doi.org/10.1002/2017JF004469
- 750 Connon, R.F., Quinton, W.L., Craig, J.R., & Hayashi, M. (2014) Changing hydrologic connectivity due to permafrost thaw in the lower Liard River valley, NWT, Canada *Hydrol Process.*, 28, 4163–78. doi.org/10.1002/hyp.10206
- Connon, R. F., Quinton, W.L., Craig, J.R., Hanisch, J., & Sonnentag, O. (2015). The hydrology of interconnected bog complexes in discontinuous permafrost terrains *Hydrol. Process.* 29, 3831-47. doi.org/10.1002/hyp.10604
- 755 DeAngelis, A., Qu, X., Zelinka, M., & Hall, A. (2015). An observational radiative constraint on hydrologic cycle intensification. *Nature*, 528, 249-253. DOI: 10.1038/nature15770
- Devoie, É.G., Craig, J.R., Connon, R.F., & Quinton, W.L. (2019). Taliks: A tipping point in discontinuous permafrost degradation in peatlands. *Water Resources Research*, 55(11), 9838-9857. doi.org/10.1029/2018WR024488
- 760 Disher, B.S. (2020). Characterising the hydrological function of treed bogs in the zone of discontinuous permafrost, M.Sc. Thesis, Wilfrid Laurier University, Waterloo, 72 pp.
- Dymond, S.F., D’Amato, A.W., Kolka, R.K., Bolstad, P.V., Sebestyen, S.D., Gill, K., & Curzon, M.T. (2019). Climatic controls on peatland black spruce growth in relation to water table variation and precipitation. *Ecohydrology*, 2137. doi.org/10.1002/eco.2137
- 765 Environment and Climate Change Canada. Adjusted and homogenized Canadian climate data. Available at: <https://www.canada.ca/en/environment-climate-change/services/climate-change/science-research-data/climate-trends-variability/adjusted-homogenized-canadian-data.html> (Accessed June 1, 2020)
- 770 Eppinga, M.B., Rietkerk, M., Wassen, M.J., & De Ruyter, P.C. (2007). Linking habitat modification to catastrophic shifts and vegetation patterns in bogs. *Plant Ecol.* 200, 53-68. doi.org/10.1007/s11258-007-9309-6
- Garon-Labreque MÉ, Léveillé-Bourret É, Higgins K and Sonnentag O. 2015. Additions to the boreal flora of the Northwest Territories with a preliminary vascular flora of Scotty Creek. *Can. Field-Nat.* 129, 349–67. dx.doi.org/10.22621/cfn.v129i4.1757
- 775 Gibson, C.M., Chasmer, L.E., Thompson, D.K., Quinton, W.L., Flannigan, M.D., & Olefeldt, D. (2018). Wildfire as a major driver of recent permafrost thaw in boreal peatlands, *Nature Communications*, 9, 3041. doi.org/10.1038/s41467-018-05457-1



- 780 Haynes, K.M., Connon, R.F. & Quinton W.L. (2018). Permafrost thaw induced drying of wetlands at Scotty Creek, NWT, Canada. *Environmental Research Letters*, 13. doi.org/10.1088/1748-9326/aae46c
- Haynes, K.M., Connon, R.F. & Quinton, W.L. (2019). Hydrometeorological measurements in peatland-dominated, discontinuous permafrost at Scotty Creek, Northwest Territories, Canada. *Geosci Data J.*, 6, 85–96. doi.org/10.1002/gdj3.69
- 785 Haynes, K.M., Smart, J., Disher, B., Carpino, O. & Quinton, W.L. (Under review). The role of hummocks in re-establishing black spruce forest following permafrost thaw. Submitted to *Ecohydrology*, Manuscript ID: ECO-20-0084.
- Hayashi, M., Quinton, W. L., Pietroniro, A., & Gibson, J. J. (2004). Hydrologic functions of wetlands in a discontinuous permafrost basin indicated by isotopic and chemical signatures. *Journal of Hydrology*, 296, 81-97. doi.org/10.1016/j.jhydrol.2004.03.020
- 790 Helbig, M., Pappas, C. & Sonntag, O. (2016a). Permafrost thaw and wildfire: Equally important drivers of boreal tree cover changes in the Taiga Plains, Canada. *Geophysical Research Letters*, 43, 1598-1606. doi.org/10.1002/2015GL067193
- 795 Helbig, M., Wischnewski, K., Kljun, N., Chasmer, L.E., Quinton, W.L., Detto, M. & Sonntag, O. (2016b). Regional atmospheric cooling and wetting effect of permafrost thaw-induced boreal forest loss. *Glob Change Biol*, 22, 4048-4066. doi.org/10.1111/gcb.13348
- Holloway, J.E. & Lewkowicz, A.G. (2019). Half a century of discontinuous permafrost persistence and degradation in western Canada. *Permafrost and Periglac Process.*, 31, 85-96. doi.org/10.1002/ppp.2017
- 800 Iversen, C.M., Childs, J., Norby, R.J., Ontl, T.A., Kolka, R.K., Brice, D.J., McFarlane, K.J. & Hanson, P.J. (2018). Fine-root growth in a forested bog is seasonally dynamic, but shallowly distributed in nutrient-poor peat. *Plant Soil*, 424, 123-143. doi.org/10.1007/s11104-017-3231-z
- 805 Ketteridge, N., Thompson, D. K., Bombonato, L., Turetsky, M. R., Benscoter, B. W., Waddington, J. M. (2013). The ecohydrology of forested peatlands: simulating the effects of tree shading on moss evaporation and species composition. *Journal of Geophysical Research – Biogeosciences*, 118, 422-435. doi.org/10.1002/jgrg.20043
- 810 Kokelj, S.V., Palmer, M.J., Lantz, T.C. & Burn, C.R. (2017). Ground Temperatures and Permafrost Warming from Forest to Tundra, Tuktoyaktuk Coastlands and Anderson Plain, NWT, Canada. *Permafrost and Periglacial Processes*, 28, 543– 551. doi.org/10.1002/ppp.1934
- 815 Korosi, J.B., Thienpont, J.R., Pisaric, M.F.J., deMontigny, P., Perreault, J.T., McDonald, J., Simpson, M.J., Armstrong, T., Kokelj, S.V., Smol, J.P., & Blais, J.M. (2017). Broad-scale lake expansion and flooding inundates essential wood bison habitat, *Nature Communications*, 8, 14510. doi.org/10.1038/ncomms14510
- Kurylyk, B., Hayashi M., Quinton W., McKenzie J., & Voss C. (2016). Influence of vertical and lateral heat transfer on permafrost thaw, peatland landscape transition, and groundwater flow. *Water Resources Research*, 52 (2), 1286-1305. doi.org/10.1002/2015WR018057



- 820 Kwong, J. T. & Gan, T. Y. (1994). Northward migration of permafrost along the Mackenzie Highway and climatic warming. *Climate Change*, 26, 399-419. doi.org/10.1007/BF01094404
- Lieffers, V. J. & Rothwell, R.L. (1987). Rooting of peatland black spruce and tamarack in relation to depth of water table. *Canadian J. Bot.* 65, 817-821.
- 825 Loisel, J. & Yu, Z. (2013). Surface vegetation patterning controls carbon accumulation in peatlands. *Geophysical Research Letters*, 40, 5508-5513. doi.org/10.1002/grl.50744
- Mekis, É & Vincent, L.A. (2011). An overview of the second generation adjusted daily precipitation dataset for trend analysis in Canada. *Atmosphere-Ocean*, 49(2), 163-177. doi.org/10.1080/07055900.2011.583910
- 830 Natural Resources Canada (2017). Wooded areas, saturated soils and landscape in Canada – CanVec series – Land features. Available at: <https://open.canada.ca/data/en/dataset/80aa8ec6-4947-48de-bc9c-7d09d48b4cad> (Accessed July 10, 2019)
- 835 Olefeldt, D., Goswami, S., Grosse, G., Hayes, D., Hugelius, G., Kuhry, P., McGuire, A.D., Romanovsky, V.E., Sannel, A.B.K., Schuur, E.A.G. & Turetsky, M.R. (2016). Circumpolar distribution and carbon storage of thermokarst landscapes, *Nature Communications*, 7, 13043. doi.org/10.1038/ncomms13043
- Overland, J.E., Hanna, E., Hanssen-Bauer, I., Kim, S.J., Walsh, J.E., Wang, M., Bhatt, U.S., Thoman, R.L., & Ballinger, T.J. (2019): Surface Air Temperature. Arctic Report Card 2019, J. Richter-Menge, M. L. Druckenmiller, and M. Jeffries, Eds., <http://www.arctic.noaa.gov/Report-Card>.
- 840 Pelletier, N. Talbot, J., Olefeldt, D., Turetsky, M., Blodau, C., Sonnentag, O., Quinton, W.L. (2017). Influence of Holocene permafrost aggradation and thaw on the paleoecology and carbon storage of a peatland complex in northwestern Canada. *Holocene*, 27, 1391–1405. doi.org/10.1177/0959683617693899
- 845 Pomeroy, J.W., Toth, B., Granger R.J., Hedstrom N.R., & Essery R.L.H. (2003). Variation in surface energetics during snowmelt in a subarctic mountain catchment. *Journal of Hydromet.*, 4, 702-719. DOI: 10.1175/1525-7541(2003)004<0702:VISED>2.0.CO;2
- 850 Quinton, W., Berg, A., Braverman, M., Carpino, O., Chasmer, L., Connon, R., Craig, J., Devoie, É., Hayashi, M., Haynes, K., Olefeldt, D., Pietroniro, A., Rezanezhad, F., Schincariol, R., and Sonnentag, O. (2019). A synthesis of three decades of hydrological research at Scotty Creek, NWT, Canada, *Hydrol. Earth Syst. Sci.*, 23, 2015-2039. doi.org/10.5194/hess-23-2015-2019
- 855 Quinton, W. L. & Carey, S. K. (2008). Towards an energy-based runoff generation theory for tundra landscapes, *Hydrological Processes*., 22. DOI: 10.1002/hyp.7164
- Quinton, W. L., Hayashi, M., & Chasmer, L. E. (2009). Peatland hydrology of discontinuous permafrost in the Northwest Territories: overview and synthesis. *Canadian Water Resources Journal*, 34(4), 311–328. doi.org/10.4296/cwrj3404311



- 860 Quinton, W., Hayashi, M., & Chasmer, L. (2011). Permafrost-thaw-induced land- cover change in the Canadian subarctic: Implications for water resources. *Hydrological Processes*, 25, 152-158. doi.org/10.1002/hyp.7894
- Quinton, W.L., Hayashi, M. & Pietroniro, A. (2003), Connectivity and storage functions of channel fens and flat bogs in northern basins. *Hydrol. Process.*, 17, 3665-3684. doi.org/10.1002/hyp.1369
- 865 Robinson, S.D., 2002. Peatlands of the Mackenzie Valley: Permafrost, Fire, and Carbon Accumulation. In: Long-Term Dynamics...Z.C. Yu et al. (eds.). Proc. of Int. Workshop on Carbon Dynamics of Forested Peatlands: Knowledge Gaps, Uncertainty and Modelling Approaches. 23-24 March, 2001, Edmonton, Canada, 21-24.
- 870 Robinson, S. D., & Moore, T. R. (2000). The influence of permafrost and fire upon carbon accumulation in high boreal peatlands, Northwest Territories, Canada. *Arctic, Antarctic, and Alpine Research*, 32(2), 155–166. doi.org/10.1080/15230430.2000.12003351
- Schuur, T., (2019) Permafrost and the Global Carbon Cycle. Arctic Report Card 2019, J. Richter-Menge, M. L. Druckenmiller, and M. Jeffries, Eds., <http://www.arctic.noaa.gov/Report-Card>.
- 875 Smith, S.L., Burgess, M.M., Riseborough, D. & Nixon, F.M. (2005). Recent trends from Canadian permafrost thermal monitoring network sites. *Permafrost and Periglacial Process*. 16, 19-30. DOI: 10.1002/ppp.511
- Smith, S.L., Burgess, M.M., Riseborough, D.W. (2008). Ground temperature and thaw settlement in frozen peatlands along the Norman Wells pipeline corridor, NWT Canada: 22 years monitoring. *Ninth International Conference on Permafrost*, 1665-1670.
- 880 Smith, S.L. & Riseborough, D.W. (2010). Modelling the thermal response of permafrost terrain to right-of-way disturbance and climate warming. *Cold Regions Science and Technology*, 60, 92-103. <https://doi.org/10.1016/j.coldregions.2009.08.009>
- 885 St. Jacques, J.M. & Sauchyn, D.J. (2009). Increasing winter baseflow and mean annual streamflow from possible permafrost thawing in the Northwest Territories, Canada. *Geophysics Research Letters* 36. doi.org/10.1029/2008GL035822
- Tarnocai, C. (2009) The impact of climate change on Canadian peatlands *Can. WaterRes. J.*, 34, 453-66. doi.org/10.4296/cwrj3404453
- 890 Thie, J. (1974). Distribution and thawing of permafrost in the southern part of the discontinuous permafrost zone in Manitoba. *Arctic Journal of the Arctic Institute of North America*, 34(3), 189-200. doi.org/10.14430/arctic2873
- Vincent, L.A., Wang, X.L., Milewska, E.J., Wan, H., Yang, F., & Swail, V. (2012). A second generation of homogenized Canadian monthly surface air temperature for climate trend analysis. *Journal of Geophysical Research*, 117, pp 13. doi.org/10.1029/2012JD017859
- 895 Vincent, L., Zhang, X., Brown, R., Feng, Y., Mekis, E., Milewska, E., Wan, H., & Wang, X. (2015). Observed trends in Canada’s climate and influence of low-frequency variability modes, *Journal of Climate*, 28. doi.org/10.1175/JCLI-D-14-00697.1



- 900 Vitt, D. H., Halsey, L. A., & Zoltai, S. C. (1994). The bog landcovers of continental Western
Canada in relation to climate and permafrost patterns. *Arctic and Alpine Research*, 26(1),
1– 13. DOI: 10.1080/00040851.1994.12003032
- Walvoord, M.A., Voss, C.I., Ebel, B.A. & Minsley, B.J. (2019) Development of perennial thaw
zones in boreal hillslopes enhances potential mobilization of permafrost carbon, *Environ.
Res. Lett.* 14. doi.org/10.1088/1748-9326/aaf0cc
- 905 Warren, R.K., Pappas, C., Helbig, M., Chasmer, L.E., Berg, A.A., Baltzer, J.L., Quinton, W.L.,
& Sonnetag, O. (2018). Minor contribution of overstory transpiration to landscape
evapotranspiration in boreal permafrost peatlands, *Ecohydrology* 11, 1975.
doi.org/10.1002/eco.1975
- Webster, C. Rutter, N., Zahnner, F. & Jonas, T. (2016). Measurement of Incoming Radiation
below Forest Canopies: A Comparison of Different Radiometer Configurations. *J.
910 Hydrometeor.* 17, 853–864. doi.org/10.1175/JHM-D-15-0125.1
- Wright, N., Hayashi, M., & Quinton, W. (2009). Spatial and temporal variations in active layer
thawing and their implication on runoff generation in peat-covered permafrost terrain.
Water Resources Research, 45(5). doi.org/10.1029/2008WR006880
- 915 Zoltai, S. C., & Tarnocai, C. (1975). Perennially frozen peatlands in the Western Arctic and
Subarctic of Canada. *Canadian Journal of Earth Science*, 12, 28–43.
doi.org/10.1139/e75-004
- Zoltai, S. C. (1993). Cyclic development of permafrost in the peatlands of Northwestern Alberta,
Canada. *Arctic Alpine Research*, 25, 240–6. DOI: 10.1080/00040851.1993.12003011